Journal of Alloys and Compounds 480 (2009) 76–80

Contents lists available at ScienceDirect

Journal of Alloys and Compounds

journal homepage: www.elsevier.com/locate/jallcom

High-pressure high-temperature phase transition of γ′-Fe_4N

R. Niewa [a,*], D. Rau [a], A. Wosylus [b], K. Meier [b], M. Wessel [c], M. Hanfland [d], R. Dronskowski [c], U. Schwarz [b]

[a] Department Chemie, Technische Universität München, Lichtenbergstraße 4, 85474 Garching, Germany
[b] Max-Planck-Institut für Chemische Physik fester Stoffe, Nöthnitzer Straße 40, 01187 Dresden, Germany
[c] Institut für Anorganische Chemie, Landoltweg 1, RWTH Aachen University, 52056 Aachen, Germany
[d] European Synchrotron Radiation Facility, 6 rue Jules Horowitz, BP220, 38043 Grenoble, France

ARTICLE INFO

Article history:
Received 16 July 2008
Received in revised form
17 September 2008
Accepted 19 September 2008
Available online 20 November 2008

PACS:
61.05.cp
61.66.Fn
61.50.Ks

Keywords:
Nitride materials
Crystal structure
High-pressure

ABSTRACT

High-temperature high-pressure treatment of γ′-Fe_4N at 1600 K and 15 GPa in a two-step multi-anvil module integrated in a uniaxial press leads to a phase transition concomitant to a re-crystallization of the nitride material in a hexagonal ε-type arrangement. Single crystals of ε-$Fe_3N_{0.95(2)}$ with $a = 4.6828(2)$ Å, $c = 4.3705(2)$ Å, $V = 83.000(6)$ Å^3, $Z = 2$) were obtained. A structural model of iron atoms in the motif of a hexagonal close packing with occupation of octahedral voids by nitrogen exhibiting long-range order was constructed and refined on the basis of X-ray diffraction data revealing a nitrogen deficiency $x = 0.05(2)$. Two likely structural order models of nitrogen in the space groups $P312$ ($R(F) = 0.024$, $wR(F^2) = 0.030$) and $P6_322$ ($R(F) = 0.021$, $wR(F^2) = 0.023$) are discussed. By means of density-functional electronic-structure calculations a pressure-induced phase transition is predicted for Fe_4N from $Pm\bar{3}m$ to $P312$ at about 6 GPa at 0 K, which also offers an interpretation for the reaction mechanism on the basis of the experimental data.

1. Introduction

γ′-Fe_4N is the iron-richest stable phase in the binary system iron–nitrogen. This and other binary iron nitride phases such as ε-Fe_3N and ζ-Fe_2N have particular impact as hard, corrosion and wear resistant surface layers of iron and steel workpieces. Not surprisingly, a large number of scientific research projects are devoted to the determination of the mechanical properties of iron nitrides and their dependence on both the nitrogen content and properties like microstructure or chemical composition of the initial steel material. However, all previous investigations were carried out on either microcrystalline powders of nitridated pure iron or hard microcrystalline layers of steel workpieces. High-pressure investigations on binary iron nitrides are rare at best. Fig. 1 shows a representation of the generally accepted phase diagram Fe–N [1,2]. Next to solution phases of nitrogen in Fe it contains the nitrides γ′-Fe_4N, ε-Fe_3N and ζ-Fe_2N. γ′-Fe_4N and ζ-Fe_2N exhibit only narrow homogeneity ranges, whereas ε-Fe_3N covers a large range of compositions at higher temperatures. It should be noted that the depicted phase diagram is a non-equilibrium diagram, i.e., at elevated temperatures, nitrogen loss and thus changes in the composition occur, as the equilibrium nitrogen pressure above the nitride phase is usually not reached under normal conditions.

For γ′-Fe_4N in earlier *in situ* high-pressure X-ray diffraction studies performed on a two-phase sample consisting of γ′-Fe_4N and ε-Fe_3N_{1+x}, it was observed that the diffraction intensities vanish near 30 GPa [3]. The authors interpreted this observation as either due to the occurrence of a phase transition or a pressure-induced disorder in the crystal structure. However, they noted that a transition to an ε-type crystal structure would not be obvious, since the reflections were covered by the second initial phase. An *in situ* X-ray magnetic circular dichroism study of γ′-Fe_4N up to 11 GPa [4] and two *in situ* Mößbauer spectroscopy investigations [5,6] up to 12 GPa all revealed a pressure-induced demagnetization which also may indicate a phase transition. However, no structural change was observed up to 8 GPa in energy-dispersive X-ray diffraction experiments [4].

Here we present, for the first time, a successful crystal growth of a pure binary iron nitride. Starting with γ′-Fe_4N we have obtained single crystals of ε-Fe_3N as a result of a phase-transition reaction followed by crystallization at high pressures.

* Corresponding author.
E-mail address: rainer.niewa@mytum.de (R. Niewa).

0925-8388/$ – see front matter © 2008 Elsevier B.V. All rights reserved.
doi:10.1016/j.jallcom.2008.09.178

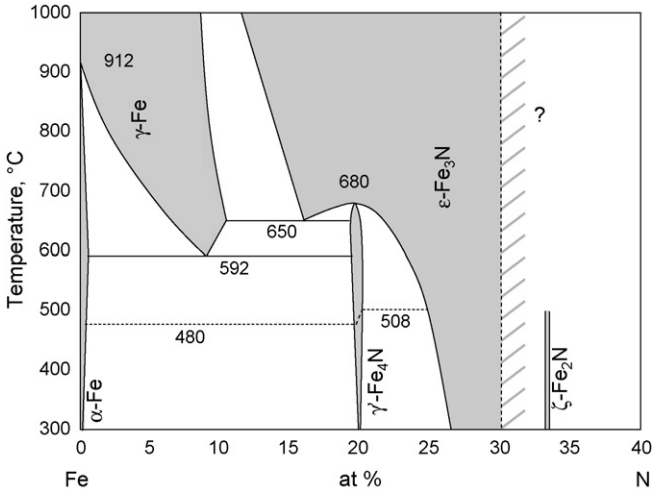

Fig. 1. Phase diagram of the binary system Fe–N according to literature [1,2].

2. Experimental

2.1. Precursor preparation and characterization

Pure microcrystalline γ′-Fe_4N was prepared from the reaction of iron powder (99.9%, Johnson Matthey/Alfa) in a mixture of flowing NH_3 (99.98%, 30 sccm) and H_2 (99.999%, 30 sccm) at 793 K (sccm = gas volume flow per minute in cm^3 at standard conditions).

Chemical analyses with regard to nitrogen and hydrogen were performed using the carrier gas hot-extraction technique on a LECO analyzer TCH-600. All values are averages of at least three independent measurements. Chemical analysis of the starting material results in the composition of $Fe_4N_{0.995(5)}$. Hydrogen analysis resulted in a concentration below the detection limit of 0.008% for the selected sample weights.

2.2. Ex situ high-pressure crystal growth and characterization

High-pressure conditions are realized using a hydraulic uniaxial press, and force redistribution in order to achieve quasi-hydrostatic conditions is accomplished by a Walker-type module (two-stage assembly with a central octahedral pressure chamber) and MgO/Cr_2O_3 octahedra with an edge length of 14 or 18 mm. Elevated temperatures are accomplished by resistive heating of graphite tubes encapsulating the sample crucible machined from hexagonal BN. Pressure and temperature calibration is completed before the experiments by analyzing the resistance changes of bismuth and lead [7] and measuring set-ups equipped with a thermocouple, respectively.

A typical high-pressure synthesis of bulk single-crystalline material requires pressure increase within 5 h to 15(2) GPa, holding at the maximal pressure for typically 5 h followed by decompression within 10 h. At the maximum pressure samples were heated at 1600(200) K for 5 min. Heated samples are quenched to ambient temperature by disconnecting the heating current before pressure release. Products were grayish-black compact cylindrical ingots. Larger crystalline, irregularly shaped particles with typical edge-length of 20 μm exhibit a grayish-black metallic luster. Data collection was performed after selecting the best of five tested crystals by means of a Rigaku R-axis spider diffractometer equipped with a rotating anode (Ag Kα radiation) and an imaging plate detector.

3. Theoretical methods

The *ab initio* calculations were based on the plane wave/pseudopotential strategy using the computer program VASP (Vienna *Ab-Initio* Simulation Package) [8,9] employing the generalized gradient approximation (GGA) of PBE type [10] and the projected-augmented wave (PAW) method [11]. For comparison, selected calculations were repeated using ultra-soft pseudopotentials of Vanderbilt type [12]. A cut-off energy of 500 eV and a dense net of *k*-points was chosen to find the optimum structure lying lowest in energy. For a correct simulation of Fe_4N in space group *P*312 the supercell approach was used. To do so, a unit cell of ε-Fe_3N was doubled both in *x* and *y* directions and two nitrogen atoms were carefully removed such as to yield the correct composition but conserve the *P*312 symmetry. It seems that this structural model bears similarities with the original model depicted by Jack [13] despite the fact that the exact symmetry of Jack's model has not been specified in detail. All cells were allowed to change in volume and shape, and all atomic positions were allowed to relax, too. Because of the small energy differences the convergence criterion of the electronic-structure calculation was set to 0.01 meV. After finding the cell lowest in energy for each structure, the volume was changed somewhat around the equilibrium volume. The bulk modules were obtained by fitting a Murnaghan-type equation of state to the energy–volume data.

4. Results and discussion

Treatment of γ′-Fe_4N at $p = 15(2)$ GPa and $T = 1600(200)$ K reproducibly converts the microcrystalline powder into a compact well-crystallized material in a concomitant phase transition and pressure-induced crystallization to $Fe_3N_{0.95(2)}$. No second phase is observed. The observed increase in nitrogen-to-iron ratio might

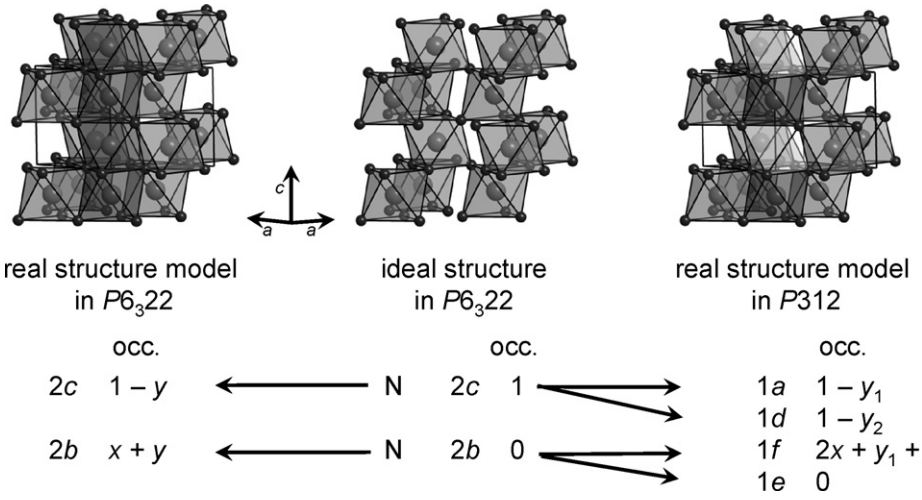

Fig. 2. Comparison of the ideal structure for ε-Fe_3N (middle) in space group $P6_322$ with the models for the real structure of the ε-phase including nitrogen site disorder and deviation from the ideal composition ε-$Fe_3N_{1\pm x}$. The parameter *x* represents the deviation from the ideal composition and *y* (or $y_1 + y_2$, respectively) gives the nitrogen transfer from site 2*c* in the idealized structure model to the additionally occupied octahedral voids.

Table 1
Crystal structure data of ε-$Fe_3N_{0.95(2)}$ for refinements in space group $P312$ and $P6_322$.

Space group refined composition	$P312$ $Fe_3N_{0.94(2)}$	$P6_322$ $Fe_3N_{0.97(2)}$
a (Å)	4.6828(2)	
c (Å)	4.3705(2)	
V (Å^3)	83.000(6)	
Z	2	
D_{calcd} (g cm^{-3})	7.231	7.245
μ(Ag K) (mm^{-1})	13.04	13.04
F(0 0 0) (e)	169.2	169.5
$h\,k\,l$ range	−7 −9, −9 −6, ±8	
$2\theta_{max}$ (°)	70.0	
Reflections measured	1629	
Reflections unique	505	255
R_{int}	0.0124	0.0131
Param. refined	20	12
R(F) ($F_0 > 4\sigma(F_0)$)	0.0157	0.0158
$R(F)$, $wR(F^2)$ (all reflections)	0.0243, 0.0298	0.0206, 0.0234
GoF (F^2)	1.084	1.283
$\Delta\rho_{max}$ (e Å^{-3})	0.72	0.59
Flack parameter	0.59(9)	0.4(1)

be due to formation of a small amount of elemental iron or a nitrogen poor phase located at the grain boundaries or due to nitrogen depletion in the boron nitride crucible material and is currently under investigation. This is the first report on a preparation of single crystals of a pure binary iron nitride, only one report on preparation of strongly Ni-doped crystals of γ′-Fe_4N can be found in literature [14,15]. X-ray powder and single crystal diffraction revealed the product to be single phase with a hexagonal unit cell and belonging to the ε-type homogeneity range of the phase diagram generally called ε-Fe_3N. The unit-cell determination from single-crystal X-ray diffraction (hexagonal, $a = 4.6828(2)$ Å, $c = 4.3705(2)$ Å compared to $a = 4.7160$ Å, $c = 4.3859$ Å for ε-$Fe_3N_{1.10}$ [16]) already indicated a composition close to the ideal composition Fe_3N. The phase transition from cubic γ′-Fe_4N to hexagonal ε-Fe_3N is indicated in the phase diagram for elevated temperatures above 950 K, however, considering the thermal instability of iron nitrides against decomposition at such temperatures we interpret the external pressure as necessary for the crystallization of ε-Fe_3N to prevent nitrogen loss. It was earlier observed in a neutron powder-diffraction study that ε-Fe_3N_{1+x} ($x = 0$, 0.10, 0.22) suffers from increasing nitrogen disorder up to temperatures of about 700 K, while the samples started to decompose at temperatures above 750 K [16,17]. The respective decomposition of γ′-Fe_4N is expected at somewhat higher temperatures.

γ′-Fe_4N is known to crystallize in an inverse perovskite structure, i.e., a cubic close packing of Fe with N occupying 1/4 of the octahedral holes in an ordered manner, such that the cubic symmetry is conserved and a framework of all vertex-sharing octahedra $NFe_{6/2}$ results [18]. The packing of Fe is realized by two crystallographically different Fe sites, one at the vertices of those octahedra, the second one exclusively coordinated by twelve Fe. The crystal structure of ε-Fe_3N is based on the motif of a hexagonal close packing of iron with nitrogen in octahedral holes. Therefore, we have to expect the phase transition to proceed in a reconstructive manner rather than in a displacement way.

Table 2
Crystal structure parameters for ε-$Fe_3N_{0.95(2)}$ for refinements in space group $P312$.

Atom	Site	x	y	z	S.O.F.	U_{eq} (Å^2)
Fe	6l	0.99394(4)	0.33251(7)	0.24999(3)	1	0.00674(4)
N(1)	1a	0	0	0	0.87(1)	0.0055(5)
N(2)	1d	1/3	2/3	1/2	0.82(1)	0.0063(5)
N(3)	1f	2/3	1/3	1/2	0.19(1)	0.010(2)[a]

[a] Refined with isotropic displacement parameter.

Table 3
Crystal structure parameters for ε-$Fe_3N_{0.95(2)}$ for refinements in space group $P6_322$.

Atom	Site	x	y	z	S.O.F.	U_{eq} (Å^2)
Fe	6g	0.33762(3)	0	0	1	0.00669(5)
N(1)	2c	1/3	2/3	1/4	0.860(9)	0.0064(4)
N(2)	2b	0	0	1/4	0.107(9)	0.010(3)[a]

[a] Refined with isotropic displacement parameter.

In contrast to the well-known binary iron nitrides γ′-Fe_4N and ζ-Fe_2N the ε-phase exhibits an extremely broad homogeneity range in the sense of ε-$Fe_3N_{1\pm x}$ (compare with phase diagram shown in Fig. 1) [18]. Nitrogen atoms exhibit long-range occupational order in octahedral holes of the motif of a hexagonal close packing of iron leading to a crystallographic unit cell enlarged by $\sqrt{3} \times \sqrt{3} \times 1$ when compared to the simple *hcp* unit cell. As discussed earlier, the two most likely order mechanisms should be described in $P6_322$ or $P312$ [13,16]. Fig. 2 visualizes the most important structural features which will be discussed below.

A hypothetical crystal structure of ε-Fe_3N (corresponding to $Fe_3N_{1\pm x}$ with $x = 0$) with an ordered arrangement of nitrogen atoms is compatible with space group $P6_322$: All nitrogen atoms occupy Wyckoff position 2c leading to a three-dimensional framework of exclusively vertex-sharing octahedra $Fe_{6/2}N$. Additional octahedral voids within the hexagonal close packing of iron are located at the Wyckoff positions 2b and 2d; both are unoccupied in this idealized structural model. Occupation of the site 2d would connect the octahedra centered by nitrogen atoms at position 2c in direction [0 0 1] by sharing faces. Therefore, it is unlikely that these are occupied due to a short distance of $c/2$ and thus a pronounced Coulomb repulsion if nitrogen is viewed as negatively charged. This also holds for a real-structure exhibiting partial disorder of nitrogen on further octahedral holes of the close packing of iron.

The structure refinements based on X-ray diffraction data of the crystals obtained by the high-temperature–high pressure treatment lead to the composition ε-$Fe_3N_{0.95(2)}$. Thus, for a real structure model we have to consider occupation of the 2c site below unity due to the composition Fe_3N_{1-x}. Additionally, due to some entropy-driven nitrogen transfer from 2c to further octahedral voids, we have to expect some N most likely in 2b. This might proceed within two likely models: In space group $P6_322$, an occupation of 2b sites leads to additional rods of face-sharing octahedra along [0 0 1] which are linked to the octahedra of the 2c position by common edges. An alternative arrangement in space group $P312$ prevents from face-sharing within the rods. The occupancy of positions due to nitrogen transfer from site 2c must be small because of the nitrogen deficiency compared to the ideal composition Fe_3N. Close inspection of the diffraction data give no evidence for reflections of the class 0 0 l with odd l, indicating $P6_322$ as correct choice rather than $P312$. However, due to small site occupation these reflections are expected to be

Table 4
Selected bond distances (Å) for ε-Fe_3N_{1+x} for refinements in space group $P312$ and $P6_322$ with estimated standard deviations in parentheses.

$P312$	d(Fe – N)/Å
Fe(1)	
–N(1)	1.9139(2)
–N(2)	1.9187(2)
–N(3)	1.8838(1)
$P6_322$	d(Fe – N)/Å
Fe(1)	
–N(1)	1.9165(1)
–N(2)	1.8835(1)

Table 5
Relative theoretical formation enthalpies, relative volumes, bulk moduli B_0 and their derivatives B_0' (at V_0) of Fe_4N; the first experimental parameter for B_0 is given in Ref. [3] whereas the second one is given in [17].

Fe_4N	ΔH (kJ/mol)	V_{rel} (Å^3)	B_0 (GPa)^1	B_0' (GPa)^1	B_0 (GPa)^2	B_0' (GPa)^2	B_0 (GPa)^{exp}
$Pm\bar{3}m$	0.0	0	165	4.59	166	3.64	155(3)/196
$P312$	10.5	−2.233	166	4.24	168	4.20	
Elements	20.4						

The first entries for the bulk moduli and their derivatives (superscript 1) refer to the PAW-PBE-GGA approach whereas the second (superscript 2) refer to the US-GGA-PP methodology.

extremely weak also in $P312$. Occupation of additional octahedral voids in both models result in occupation factors close to zero and extremely large displacement parameters. Tables 1–3 gather technical and crystallographic data and present refinement results in both space groups. For the observed occupation of additional octahedral voids in these rods of about 10% is expected to result in only minute correlations leading to extremely small ranges of local order compatible with the $P312$ symmetry. The absolute structure resulting from the refinements for both space groups taken into account is considered too poor to warrant publication since the Flack parameter is unstable [20]. Selected distances Fe–N are given in Table 4 and fall in the range of other iron nitride phases.

A quantum-theoretical analysis was performed on Fe_4N in the space groups $Pm\bar{3}m$ and $P312$ (Table 5) as well as on ε-Fe_3N in space group $P312$. As depicted in Fig. 3, it is fairly obvious that

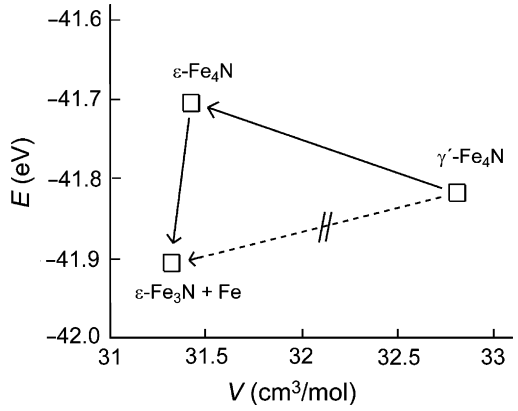

Fig. 3. Energy–volume diagram for the system ε-Fe_3N + Fe, ε-Fe_4N and γ'-Fe_4N at absolute zero temperature as calculated by density-functional theory.

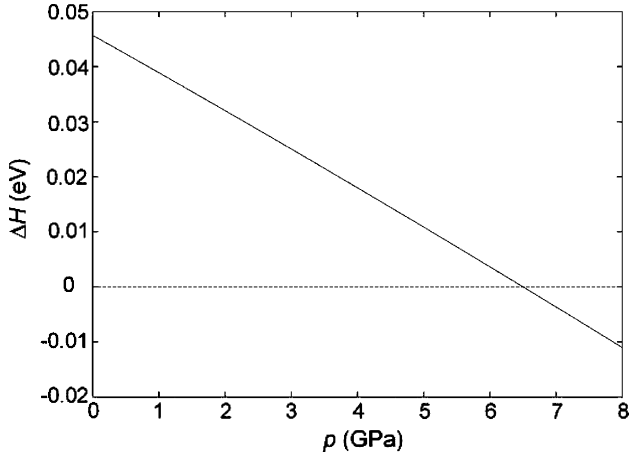

Fig. 4. Enthalpy-difference–pressure diagram for Fe_4N at absolute zero temperature as calculated by density-functional theory. While the zero line refers to the cubic $Pm\bar{3}m$ phase, the upper line refers to the hexagonal $P312$ polymorph.

cubic γ'-Fe_4N in $Pm\bar{3}m$ should spontaneously transform into ε-Fe_3N and metallic iron but this reaction has never been observed so far. Because such a phase transition will rather proceed in a reconstructive manner (see discussion above), one may safely expect a rather large activation barrier for it. Instead, we focus on an alternative reaction path via the energetically higher-lying hexagonal ε-Fe_4N (see also Fig. 3). As depicted in the figure, ε-Fe_4N in $P312$ is less stable by ΔE = 10.5 kJ/mol compared to $Pm\bar{3}m$ – like Fe_4N (i.e. γ'-Fe_4N), and the latter phase is exothermic with respect to the elements (although the formation enthalpy is theoretically slightly overestimated: −20.4 kJ/mol in $Pm\bar{3}m$ at 0 K but experimentally −11.1 kJ/mol at standard conditions [19]). Because of the differences in volume for both Fe_4N phases, however, a phase transition from cubic $Pm\bar{3}m$ into hexagonal $P312$ is predicted (Fig. 4) at about 6 GPa at 0 K, which is in reasonable agreement with the experimental values (15(2) GPa at 1600(200) K), given that the electronic-structure calculations are for zero temperature. After having arrived in the hexagonal symmetry, the phase transition from hexagonal ε-Fe_4N into likewise hexagonal ε-Fe_3N may take place by segregation of pure iron because it is an exothermic reaction (ΔE = − 18.8 kJ/mol, see also Fig. 3); in addition, the activation barrier for this reaction is small enough to let the reaction proceed.

5. Conclusions

For the first time we succeeded in the growth of pure binary iron nitride single crystals. In a high-pressure high-temperature phase transition from γ'-Fe_4N we were able to crystallize ε-$Fe_3N_{0.95(2)}$. This technique is in principle applicable for growing ε-Fe_3N phases of different composition. Inspection of the phase diagram and electronic-structure calculations reveal that the phase transition can be driven by temperature or pressure. Further investigations of the phase relations are presently in progress, and we are currently exploiting the technique aiming to gain to a deeper understanding of the order–disorder models of nitrogen in iron nitrides and the mechanical properties of single-crystalline materials.

Acknowledgements

Encouragement of Prof. Dr. Rüdiger Kniep is gratefully acknowledged. We thank Anja Völzke for performing the chemical analyses and the computing center of RWTH Aachen for providing computer resources. This work was supported by the Elitenetzwerk Bayern within the Advanced Materials Science program, the Max-Planck-Gesellschaft and within the Schwerpunktprogramm “Synthesis, ‘in situ’ characterization and quantum mechanical modeling of earth materials, oxides, carbides and nitrides at extremely high pressures and temperatures” of the Deutsche Forschungsgemeinschaft (SPP 1236).

References

[1] K.H. Jack, Proc. Roy. Soc. A 208 (1951) 200–215.
[2] H.A. Wriedt, N.A. Gokcen, R.H. Nafziger, Bull. Alloy Phase Diagrams 8 (1987) 355.

[3] J.F. Adler, Q. Williams, J. Geophys. Res. 110 (2005) B01203.
[4] N. Ishimatsu, Y. Ohishi, M. Suzuki, N. Kawamura, M. Ito, H. Maruyama, S. Nasu, T. Kawakami, O. Shimomura, Nucl. Inst. Meth. Phys. Res. A 467–468 (2001) 1061–1064.
[5] C.L. Yang, M.M. Abd-Elmeguid, H. Micklitz, G. Michels, J.W. Otto, Y. Kong, D.S. Xue, F.S. Li, J. Magn. Magn. Mater. 151 (1995) L19–L23.
[6] F. Li, Y. Kong, R. Zhou, C.L. Yang, M.M. Abd-Elmeiguid, G. Michels, H. Micklitz, J.W. Otto, Solid State Commun. 95 (1995) 753–757.
[7] D.A. Young, Phase Diagrams of the Elements, University of California Press, Berkeley, 1991.
[8] G. Kresse, J. Furthmüller, Comput. Mater. Sci. 6 (1996) 15;
G. Kresse, J. Furthmüller, Phys. Rev. B 55 (1996) 11169–11186.
[9] G. Kresse, J. Hafner, Phys. Rev. B 47 (1993) 558–561;
G. Kresse, J. Hafner, Phys. Rev. B 49 (1994) 14251–14269.
[10] J.P. Perdew, K. Burke, M. Ernzerhof, Phys. Rev. Lett. 77 (1996) 3865–3868.
[11] P.E. Blöchl, Phys. Rev. B 50 (1994) 17953–17979.
[12] D. Vanderbilt, Phys. Rev. B 32 (1985) 8412–8415.
[13] K.H. Jack, Acta Crystallogr. 5 (1952) 404–411.
[14] H. Jacobs, J. Bock, J. Less Common Met. 134 (1987) 215–220.
[15] H. Jacobs, D. Rechenbach, U. Zachwieja, J. Alloys Compd. 227 (1995) 10–17.
[16] A. Leineweber, H. Jacobs, F. Hüning, H. Lueken, W. Kockelmann, J. Alloys Compd. 316 (2001) 21–38.
[17] A. Leineweber, H. Jacobs, F. Hüning, H. Lueken, H. Schilder, W. Kockelmann, J. Alloys Compd. 288 (1999) 79–87.
[18] K.H. Jack, Proc. Roy. Soc. A 195 (1948) 34–41.
[19] R. Blachnik, D'Ans & Lax: Taschenbuch für Chemiker und Physiker, Teil 3, Springer, Berlin, Heidelberg, New York, 1998.
[20] H.D. Flack, G. Bernadelli, J. Appl. Crystallogr. 33 (2000) 1143–1148.